TWENTYFIFTH EUROPEAN ROTORCRAFT FORUM

Paper n° C3

A PARAMETRIC STUDY OF THE AERODYNAMICS OF INPLANE MOTION

BY

S. T. SHAW, N. QIN
CRANFIELD UNIVERSITY,
UNITED KINGDOM

SEPTEMBER 14-16, 1999
ROME
ITALY

ASSOCIAZIONE INDUSTRIE PER L'AEROSPAZIO, I SISTEMI E LA DIFESA
ASSOCIAZIONE ITALIANA DI AERONAUTICA ED ASTRONAUTICA

A Parametric Study of the Aerodynamics of In-plane Motion

Scott Shaw and Ning Qin

Flow Prediction & Control,
Cranfield College of Aeronautics,
Bedford, United Kingdom.

Abstract

A computational analysis is performed of the unsteady aerodynamics associated with the blade sections of non-lifting helicopter rotors in forward flight. The unsteady flow is studied through solutions of the two-dimensional Reynolds averaged Navier-Stokes equations together with a strongly coupled two-equation model of turbulence. Two motions are studied.

The first motion is that of an aerofoil subjected to harmonic in-plane oscillations. The influence of advance ratio and reduced frequency is investigated. It is shown that, in the absence of shock waves, the flow is periodic with a reduced frequency equal to that of the forcing motion. However, the flow development lags behind the forcing motion. Furthermore, for constant reduced frequency the phase lag is independent of advance ratio.

In addition to harmonic motion, the aerodynamic response to a step change in Mach number is investigated. Using an assumed form of the indicial response, a lift transfer operator for step changes in Mach number is obtained in the Laplace domain. An analytical expression for the response to harmonic Mach number oscillations is then obtained from the transfer operator. The resulting formulation for the aerodynamic response confirms that the lag between the forcing motion and aerodynamic response is independent of advance ratio.

1. Introduction

Despite considerable work over the last century, the accurate simulation of the flow around helicopter rotors in forward flight continues to present a significant problem for the helicopter engineer. The flow is highly unsteady and contains regions in which quite different physical mechanisms dominate the flow development. The advancing blade tip operates at high, typically transonic, Mach numbers and low lift coefficient. Conversely, on the retreating side the blades experience high lift at more modest Mach numbers. In addition, there are local regions of high loading due to strong interactions of the blade with the wake system and tip vortices of preceding blades. The situation is further complicated because of the strong coupling between the blade aerodynamics and blade motion.

In principal the Navier-Stokes equations contain all of the physics that are required to accurately represent the complex nature of these phenomena and can be coupled with structural models of the rotor system[1]. However, such a direct approach has the disadvantage that it is very computer intensive especially considering the complex nature of the phenomena which must be resolved.

In order to understand more fully the basic physical aspects of such flows it is convenient to consider simplified representations of the rotor aerodynamics. If the helicopter rotor is conceived as a very high aspect ratio wing (typical aspect ratios for a single blade are in excess of 15) then it is possible to justify the use of a two-dimensional approximation[17]. The blade loads can then be calculated by the use of a strip theory in which the local aerodynamic loading obtained for a number of discrete elements is integrated across the span. The unsteady loading at each of the spanwise stations is obtained using the local flow conditions. For a two-dimensional blade section the local variation of incidence and Mach number over one complete revolution of the rotor can be described by equations of the form,

$$\alpha(t) = \sum_{n=1}^{\infty} \left(A_n \cos(2\pi nkt) + B_n \sin(2\pi nkt) \right) \qquad (1)$$

and

$$U(t) = U_0 \left(1 + \mu \sin(2\pi kt) \right) \qquad (2)$$

Today we understand well the qualitative and quantitative behaviour of the aerodynamics of aerofoils that are oscillated about the pitch axis. This has largely been due to careful observation and measurement of wind tunnel experiments. In contrast, we have only a rudimentary understanding of the aerodynamic behaviour due to the unsteady variation of Mach number, although such behaviour dominates the advancing blade in high-speed forward flight.

The influence of such oscillations on the low speed aerodynamics of aerofoils at high lift was studied experimentally by Maresca et al[2], Krause and Schweitzer[3] and Ho et al[4-6]. Subsequently, Morinishi[7] presented numerical solutions of the incompressible Navier-Stokes equations for this problem. While such investigations are of considerable interest, they have mainly served to demonstrate the influence of in-plane motion at very

low Mach numbers and high angles of attack. While this provides insight into the dynamic stall process on the retreating blade, the flow conditions studied provide no information about the influence of dynamic effects on the advancing blade.

Szumowski[8] investigated the effect of background flow oscillations in the transonic flow regime. The oscillations were generated by means of a rotating plate placed downstream of the aerofoil. It was shown that the transonic aerodynamics of aerofoils is sensitive to external excitation of the flow. For low amplitude oscillations, the shock dynamics were characterised as Tidjeman Type B[9], however for sufficiently high amplitudes a free shock wave was observed to propagate upstream of the aerofoil leading edge (Tidjeman Type C).

The earliest calculations of the flow around an aerofoil in a time varying freestream representative of the advancing blade problem appear to be those of Lerat and Sides[10] who solved the integral form of the Euler equations. Habibie et al[11] investigated the aerodynamics of aerofoils subjected to harmonic variations of Mach number and ramping motions (dM/dt = constant). Subsequently Pahlke et al[12,13] compared solutions of the two- and three-dimensional Euler equations at conditions representative of helicopter rotors at various forward flight speeds.

Solutions of the Navier-Stokes equations for in-plane motion were presented by Shaw and Qin[14-16] who used the thin layer Navier-Stokes equations together with the Baldwin-Lomax turbulence model. Subsequently calculations were performed with the full Reynolds averaged Navier-Stokes equations and a two-equation model of turbulence[17]. While such calculations demonstrate the importance of the unsteady shock development, no parametric investigation of in-plane motion has been reported.

In the study of transient flows, the aerodynamic response of aerofoils to sudden changes in forcing, indicial motion, is also of interest. Approximate representations of the response functions of aerofoils subjected to step changes in pitch form the basis of the modelling used by Beddoes[18] to describe the unsteady aerodynamics of helicopter rotors. While analytical models are available for aerofoils subjected to step increases in incidence and pitch rate there are no corresponding solutions for aerofoils experiencing a step increase in Mach number. Shaw and Qin[19] used numerical solutions of the Navier-Stokes equations to investigate the aerodynamics of aerofoils subjected to step changes in Mach number.

The present paper describes a parametric study of the influence of advance ratio and reduced frequency on the computed aerodynamics of in-plane motion. Furthermore, calculations of the aerodynamic response to a step change in Mach number are used to obtain a functional form of the lift transfer operator. Using the lift transfer operator and Duhamel's integral, a formulation for the lift response to harmonic variations in Mach number is deduced. This result is used to confirm the findings of the parametric study.

2. Numerical method

Governing Equations

The governing equations are the unsteady two-dimensional Reynolds averaged Navier-Stokes (RANS) equations together with a strongly coupled two-equation model of turbulence. The governing equations can be expressed in the following integral form,

$$\frac{\partial}{\partial t}\iiint_{\Omega} Q\,d\Omega + \iint_{S} F\cdot n\,dS = \iiint_{\Omega} H d\Omega \qquad (3)$$

In this equation, Q is the vector of conserved variables,

$$[\rho \quad \rho u \quad \rho v \quad \rho E \quad \rho k \quad \rho\omega]^T$$

ρ is the density of the fluid, u and v are the components of velocity in a Cartesian co-ordinate system and E is the energy of the fluid particle element,

$$E = e + \tfrac{1}{2}\left(u^2 + v^2\right) + k \qquad (4)$$

F represents the flux vector, and is made up from contributions that may be conveniently grouped together as convection and diffusion terms, denoted by the superscripts i and v respectively. The fluxes due to the convection terms may be written for a Cartesian co-ordinate system in the following form,

$$F_x^i = \begin{bmatrix} \rho\overline{U} \\ \rho u\overline{U} + P \\ \rho v\overline{U} \\ \overline{U}(\rho E + P) + u_T P \\ \rho\overline{U}k \\ \rho\overline{U}\omega \end{bmatrix} \quad F_y^i = \begin{bmatrix} \rho\overline{V} \\ \rho u\overline{V} \\ \rho v\overline{V} + P \\ \overline{V}(\rho E + P) + v_T P \\ \rho\overline{V}k \\ \rho\overline{V}\omega \end{bmatrix}$$

The contra-variant velocities are,

$$\overline{U} = u - u_T \text{ and } \overline{V} = v - v_T$$

here u_T and v_T represent the grid velocities with which the integration boundaries move. The corresponding components of the viscous flux vector are,

$$F_x^v = \begin{bmatrix} 0 \\ \tau_{xx} \\ \tau_{xy} \\ u\tau_{xx} + v\tau_{xy} - q_x \\ (\mu + \sigma_k \mu_t)\dfrac{\partial k}{\partial x} \\ (\mu + \sigma_\omega \mu_t)\dfrac{\partial \omega}{\partial x} \end{bmatrix} \quad F_y^v = \begin{bmatrix} 0 \\ \tau_{xy} \\ \tau_{yy} \\ u\tau_{xy} + v\tau_{yy} - q_y \\ (\mu + \sigma_k \mu_t)\dfrac{\partial k}{\partial y} \\ (\mu + \sigma_\omega \mu_t)\dfrac{\partial \omega}{\partial y} \end{bmatrix}$$

in which τ is the shear stress tensor, q is the heat flux vector and $\sigma_k = \sigma_\omega = 0.5$.

In order to obtain a closed mathematical system a number of auxiliary relations describing the interdependence of the thermodynamic variables are introduced. For a perfect gas the pressure, density and temperature are related to one another using Boyle's thermal equation of state,

$$P = \rho RT \tag{5}$$

in which R is the universal gas constant and T is the temperature. Density and pressure are related to one another through the internal energy e,

$$e = \frac{1}{(\gamma - 1)}\frac{P}{\rho} \tag{6}$$

in this equation γ is the ratio of specific heats.

The turbulent stresses are modelled by analogy with the molecular transport of momentum. The turbulent viscosity, μ_T, is obtained using the standard Wilcox k-ω model[20]. This model has been widely adopted by the CFD community, and has several desirable features. It is wall distance free, does not require damping functions in the viscous sub-layer and performs satisfactorily in the presence of adverse pressure gradients.

Spatial discretisation

The equations describing the evolution of the mean flow and turbulence are integrated simultaneously using the closely coupled numerical scheme developed at Cranfield University[21]. The closely coupled solver is based upon Osher and Solomon's[22] approximate Riemann solver. This algorithm is patterned after Godunov's method, but instead of computing the intercell flux exactly an approximate splitting is introduced. The numerical flux can then be calculated using,

$$\tilde{f}_{i+\frac{1}{2}} = \frac{1}{2}\left[f_i + f_{i+1} - \int_{Q_i}^{Q_{i+1}} |A(Q)| \, dQ \right] \tag{7}$$

where the integration is performed in the phase (or state) space. In Osher and Solomon's original scheme the integration was performed with a reversed ordering of the sub-curves in order to prove some analytical properties of the scheme. A more natural ordering is in the direction associated with the physical ordering of the Eigenvalues. This variant is employed in the present work.

Higher order spatial accuracy is obtained using Van Leer's MUSCL scheme[23], in which the piecewise constant initial data are replaced by linear functions of the conserved variables. In order to ensure numerical stability of the scheme a slope limiter is employed. This ensures that the scheme reverts to first order accuracy in the region of strong flow discontinuities. The spatial discretisation of the convective terms is nominally third order accurate in smooth regions of the flow.

The diffusive terms are discretised using a finite volume scheme in which the velocity gradients are calculated using Gauss's theorem. The resulting scheme is second order accurate on a smoothly varying mesh.

Temporal discretisation

Following spatial discretisation a system of ordinary differential equations is obtained that is continuos in time,

$$\frac{dQ}{dt} = -R(Q) \tag{8}$$

This system of equations is integrated using a fully implicit Newton method. A backward Euler time discretisation of the governing equations gives,

$$\frac{Q^{n+1} - Q^n}{\Delta t} + R\left(Q^{n+1}\right) = 0 \tag{9}$$

where $R(Q)$ is the spatial discretisation. This is of the general form,

$$\tilde{R}\left(Q^{n+1}\right) = 0 \tag{10}$$

and a straightforward application of Newton's method gives,

$$\frac{\partial \tilde{R}}{\partial Q^{n+1}}\left(\Delta Q^{n+1}\right)^l = -\tilde{R}\left(Q^{n+1}\right)^l \tag{11}$$

This equation is the basis of the solver PINK2e used in the current work.

The linear system Ax = b arising at each Newton step is solved using restarted GMRES[24]. In order to improve the convergence of GMRES a preconditioner based upon approximate factorisation is employed[25].

3. Representation of aerofoil motion

Harmonic motion

The normal component of Mach number for a rotor blade section located at distance r from the axis of rotation is given by,

$$M(t) = \frac{r}{R} M_{tip} \left(1 + \mu_r \, sin(\psi)\right) \qquad (12)$$

in which R is the radius of rotor blade, M_{TIP} is the tip Mach number due to the rotation of the blade, μ_r is the ratio of the forward flight speed to the rotational velocity at a spanwise station located a distance r from the rotor hub, i.e.

$$\mu_r = \frac{U_{fwd}}{\frac{r}{R} U_{tip}} = \frac{R}{r} \mu \qquad (13)$$

and ψ is the azimuth angle. The corresponding grid velocity terms are,

$$u_t = \frac{r}{R} U_{tip} \mu_r \, sin(k_r t) \text{ and } v_t = 0$$

here the reduced frequency, k_r, is obtained from,

$$k_r = \frac{\omega c_r}{U_r} = \frac{\omega c_r}{\omega r} = \frac{c_r}{r} \qquad (14)$$

in which c_r and ω are the local chord and angular velocity of the blade respectively.

Indicial motion

The Mach number variation for indicial motion is described by,

$$M(t) = \begin{cases} M & t = 0 \\ M + \Delta M & t > 0 \end{cases} \qquad (15)$$

the corresponding grid velocities are,

$$u_t = \begin{cases} 0 & t = 0 \\ \Delta U & t > 0 \end{cases} \text{ and } v_t = 0$$

4. Validation

In order to demonstrate the ability of the proposed method to accurately resolve the aerodynamics of aerofoils performing rigid body motions computations were performed for a number of test cases[17]. In this paper three test cases that demonstrate the capability of the method for the present class of problems are considered

Pitching oscillations

AGARD[26] has established a number of standard configurations for use in the development and validation of numerical methods for the prediction of aero-elastic responses and their associated unsteady aerodynamics. Case CT1, for which experimental data were collated by Landon[26], concerns the flow around a NACA 0012 aerofoil oscillating in pitch. The aerofoil is set at an incidence of α = 2.89° in a flow with a freestream Mach number of M = 0.60 and a Reynolds number of Re_c = 4.8 million and pitched about the quarter-chord point with an amplitude of $\Delta\alpha$ = 2.41° at a reduced frequency of k =0.1616. Unsteady calculations were performed on a fine grid containing 369 points in the direction around the aerofoil (250 of which were on the aerofoil surface) and 129 points in the direction normal to the aerofoil surface.

For this case Tidjeman Type B shock motion was computed. Figure (1) compares the calculated normal force and pitching moment with experimental measurements. Comparison between the computed and experimental data is considered satisfactory. The present correlation compares favourably with those obtained by other authors[27,28].

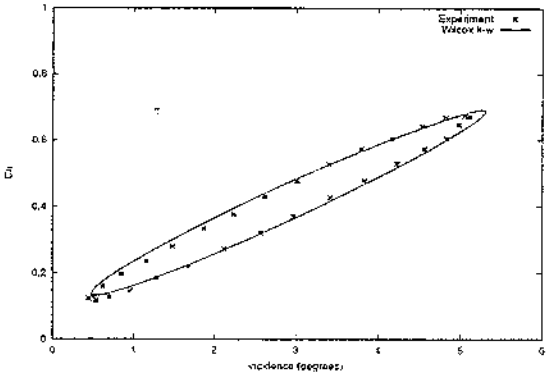

(a) Normal Force

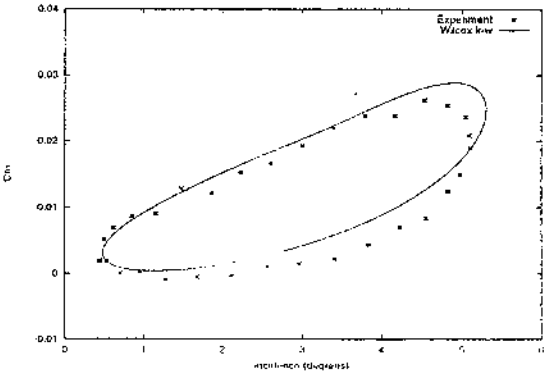

(b) Pitching Moment

Figure (1) Comparison of computed and measured forces and momnets (AGARD CT1)

In-plane motion

The second test case is that suggested by Lerat and Sides[10] for in-plane motion. Calculations were

performed for a NACA 0012 aerofoil undergoing a motion described by Equation (12) with r/R = 0.892, M_{TIP} = 0.60, μ_r = 0.61 and k_t = 0.185. The angle of incidence and Reynolds number based upon chord were $\alpha = 0°$ and Re_c = 1.75 million respectively.

In order to demonstrate the validity of the present numerical approach, the computed instantaneous pressure coefficients obtained from solution of the Euler equations are compared with the inviscid results presented by Lerat and Sides[10]. Such comparisons are considered to be satisfactory, see for example Figure (2) which shows results at x/c = 0.5.

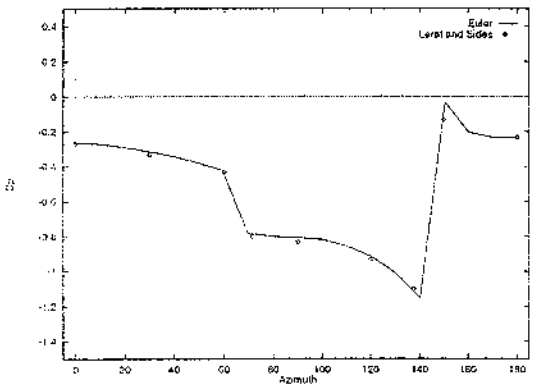

Figure (2) Comparison of the present Euler calculations with those of Lerat and Sides[10]

In Figure (3) results obtained using the two-dimensional Navier-Stokes equations and a two-equation turbulence model are compared with three-dimensional experimental measurements for a rotor blade in forward flight at x/c = 0.2 and x/c = 0.5. While the qualitative and quantitative behaviour is generally acceptable over much of the azimuth range, the development of the shock wave clearly lags that measured in the experiments. It is thought that this discrepancy arises as a consequence of significant three-dimensional effects, which cannot be represented in the current two-dimensional model. This view would seem to be supported by the results presented by Pahlke et al[13] who computed the flow around a rotor blade in forward flight using both an in-plane and full three-dimensional representation of the blade aerodynamics.

Indicial motion

A series of calculations have been performed for the response functions of an aerofoil subjected to a step increase in incidence. The initial response at time t=0.0 can be calculated from momentum considerations as,

$$\left(\frac{\Delta C_n}{\Delta \alpha}\right)_{t=0} = \frac{4}{M} \qquad (16)$$

Initial values of normal force coefficient have been extracted from the computed data and are compared with piston theory in Figure (4). From this figure it can be seen that piston theory consistently over-predicts the values obtained from the CFD calculations.

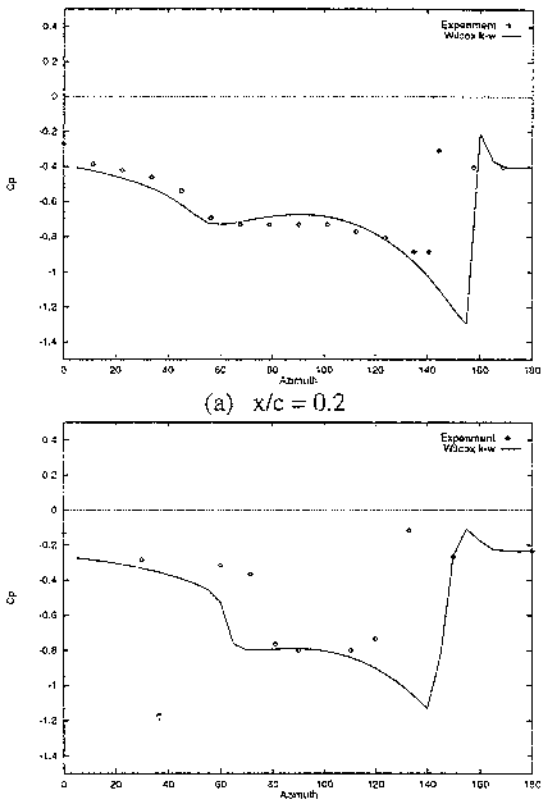

(a) x/c = 0.2

(b) x/c = 0.5

Figure (3) Comparison of in-plane calculations with three-dimensional measurements

It is likely that such discrepancies arise as a consequence of thickness effects. Singh and Baeder[29] investigated the indicial response of three-dimensional wings to step changes in incidence using solutions of the Euler equations. In their study, improved agreement was observed between linear theory and calculation when the average value of Mach number across the aerofoil chord was used instead of that of the freestream. However, for viscous flow an alternative means of determining the chordwise Mach number variation for piston theory is required as the no-slip condition requires that the velocity along the aerofoil surface is zero. For inviscid isentropic flow the local Mach number and pressure are related by,

$$\frac{P_\infty}{P} = \left(1 + \frac{\gamma - 1}{2} M^2\right)^{\frac{\gamma}{\gamma - 1}} \qquad (17)$$

in which P_∞ is the static pressure. Re-arranging this expression and integrating over the aerofoil chord we

obtain the following value for the average Mach number,

$$\tilde{M} = \int_0^1 \left[\frac{2}{\gamma - 1} \left\{ \left(\frac{P_o}{P} \right)^{\frac{\gamma-1}{\gamma}} - 1 \right\} \right]^{\frac{1}{2}} d\left(\frac{x}{c} \right) \qquad (18)$$

The agreement between values of normal force coefficient obtained using the modified piston theory and the steady Navier-Stokes solutions is much improved, see Figure (4).

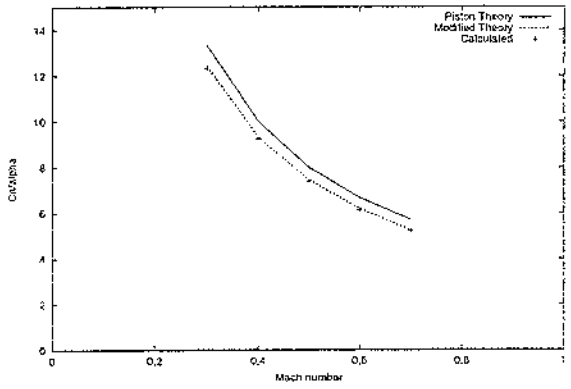

Figure (4) Comparison of computed response (t=0) with original and modified piston theorys

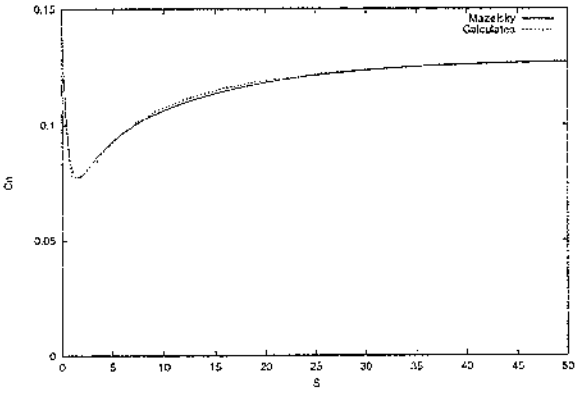

Figure (5) Comparison of computed total response with analytical solutions (M=0.5)

Approximate indicial functions for compressible flow may be derived based upon the relationship between the responses for harmonic and indicial motions. Mazelsky and Drischler[30] used numerical solutions of Poisso's equation to obtain results for the indicial lift response at Mach numbers of 0.5, 0.6 and 0.7. The results were presented in tabular form and as a three pole exponential approximation. The exponential approximation for the case M = 0.5 is compared with numerical solutions of the Navier-Stokes equations in Figure (5). Agreement between computation and theory is satisfactory. During the initial stages of the response, comparison is poor. However as shown above thickness effects on the impulsive contribution are significant (the theoretical values are for a flat plate). The latter stages of the response are well predicted using the current method.

5. Results

5.1 Harmonic motion

For a non-lifting rotor in forward flight, the blade section aerodynamics are determined by four main parameters; the reduced frequency, advance ratio, tip Mach number and Reynolds number. Typically the rotational speed of the rotor, and hence M_{TIP} and Re_c, is fixed and therefore only the advance ratio and reduced frequency were investigated. For the purposes of the present work values of $M_{TIP} = 0.5113$, $Re_c = 1.75$ million and $\alpha = 0°$ were employed. Calculations were performed for combinations of four different advance ratios and three different reduced frequencies, see Table (1) for further details.

Case	μ_r	k_r
1	0.2000	0.050
2	0.3000	0.050
3	0.4000	0.050
4	0.5263	0.050
5	0.2000	0.095
6	0.3000	0.095
7	0.4000	0.095
8	0.5263	0.095
9	0.2000	0.150
10	0.3000	0.150
11	0.4000	0.150
12	0.5263	0.150

Table (1) Flow conditions

The calculations were performed on a grid containing 369 points in the direction around the aerofoil and 129 points in the direction normal to the aerofoil surface. A time step equivalent to 1/4° of azimuth (1440 steps/revolution) was employed. Typically, a converged periodic solution was computed within the first cycle of the aerofoil motion, however the data discussed are taken from the third cycle.

Advance ratio

In Figure (6), the development of the unsteady flow is revealed through contours of instantaneous local surface pressure coefficient (note that for the purposes of this figure pressure coefficient is defined in terms of the local instantaneous freestream velocity). Results are shown for a constant reduced frequency of $k_r = 0.095$. The results presented for an advance ratio of $\mu_r = 0.20$ are typical of those obtained

for shock free flows. For this case, the effects of flow unsteadiness are not appreciable. Flow unsteadiness is confined mainly to the region between the quarter and mid-chord points, forward and aft of this region the pressure contours are parallel to the leading edge indicating that the flow behaves in a quasi-steady manner. The flow is periodic with a time period identical to that of the forcing motion. The computed periodic response is first harmonic in character, but lags the forcing motion.

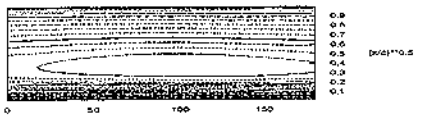

(a) $\mu' = 0.2000$

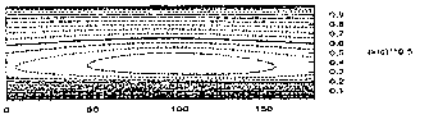

(b) $\mu' = 0.3000$

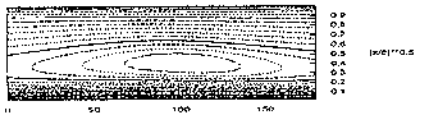

(c) $\mu' = 0.4000$

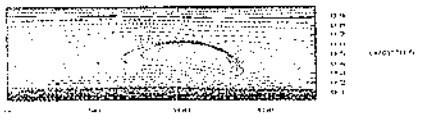

(d) $\mu' = 0.5236$

Figure (6) Development of surface pressure contours with advance ratio (k=0.095)

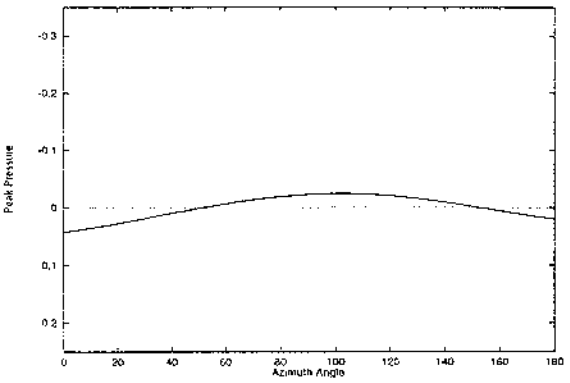

(a) $\mu' = 0.2000$

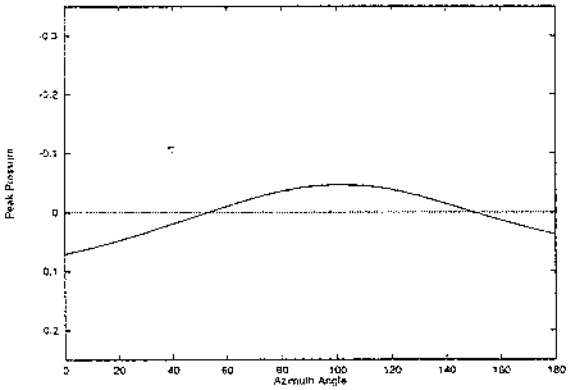

(b) $\mu' = 0.3000$

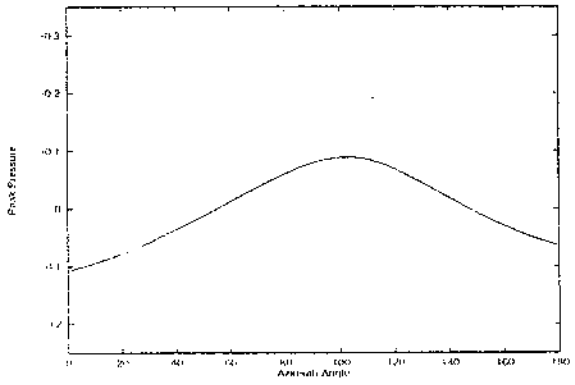

(c) $\mu' = 0.4000$

Figure (7) Unsteady development of maximum suction pressure (k=0.095)

The pressure contours plotted for $\mu_r = 0.3$ and $\mu_r = 0.4$, Figures (6b) and (6c) respectively, show similar behaviour, although it can be seen that the extent of the region over which unsteady effects are apparent increases with increasing advance ratio. The behaviour of the computed pressure contours at an advance ratio of $\mu_r = 0.5236$, Figure 6(d), is clearly different from that observed in the previous figures. While the flow response remains periodic with a time-period corresponding to that of the forcing motion, the flow response is no longer first harmonic in character. For this case, the maximum Mach number attained during the unsteady motion is sufficiently high for shock waves to appear in the flow. Furthermore, as the

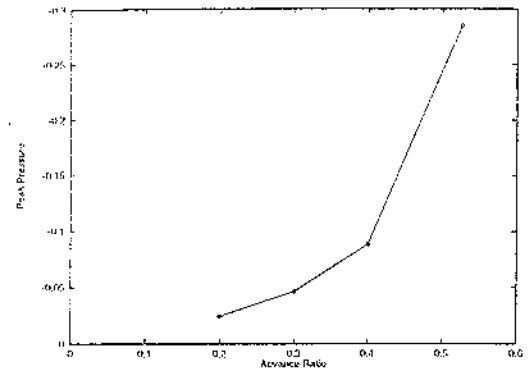

Figure (8) Behaviour of maximum peak pressure with advance ratio (k=0.095)

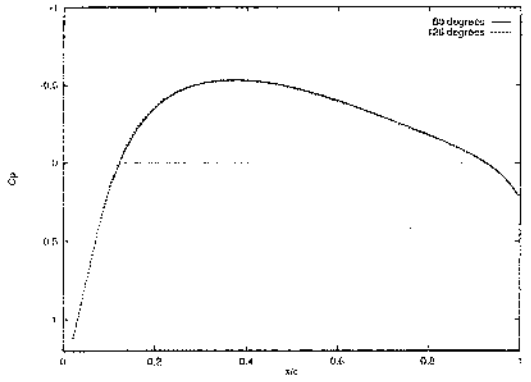

(a) $\mu' = 0.20$

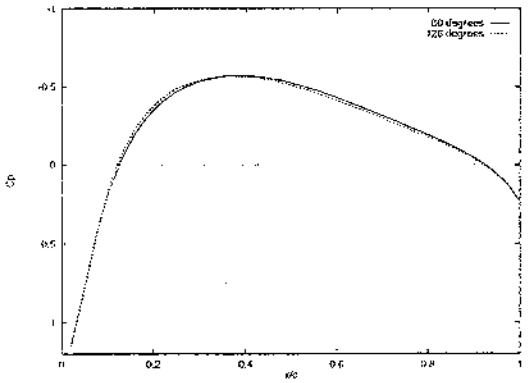

(b) $\mu' = 0.30$

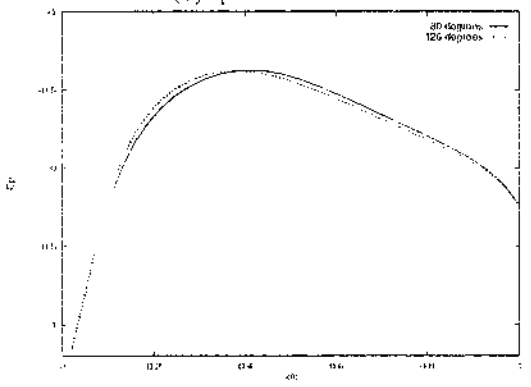

(c) $\mu' = 0.40$

Figure (9) Comparison of pressure distributions at symmetric azimuth angles (k=0.095)

incoming flow decelerates boundary layer separation is observed.

The pressure data presented in Figure (6) suggest that, in the absence of shock waves, the flow response to harmonic forcing can be described by a simple phase lag. This is demonstrated more clearly in Figure (7) in which the unsteady behaviour of peak-suction pressure coefficient is plotted against azimuth angle for each of the advance ratios considered. The behaviour of peak-suction pressure coefficient with azimuth angle is regular, and the phase lag at each advance ratio may be easily obtained. For the present data, the phase lag corresponds to an azimuth angle of 13° for each of the three advance ratios. The peak pressure coefficient is plotted in Figure (8).

Computed pressure distributions at azimuth angles symmetric about $\psi = 90° + \phi$ are plotted in Figure (9) for advance ratios of $\mu_r = 0.20$, 0.30 and 0.40, which seem to further demonstrate that the subsonic flow can be described by a simple phase lag

Reduced frequency

The influence of reduced frequency on the computed response to harmonic excitation was also investigated. For the lower advance ratios, the computed flow behaviour is similar to that described in the previous section for $k_r = 0.095$, the flow response is first harmonic in character and lags the forcing motion. The phase lag remains independent of the advance ratio, but increases with increasing reduced frequency, see Figure (10).

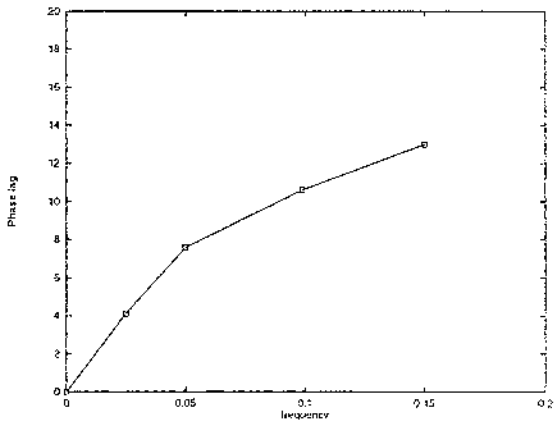

Figure (10) Influence of reduced frequency on the computed phase-lag

For advance ratios sufficiently high that supercritical flow appears for part of the cycle the influence of reduced frequency on the computed response is more pronounced. In Figure (11) instantaneous pressure distirbutions are plotted for several azimuth angles. The most obvious effect of flow unsteadiness here is that the azimuth angle at which the shock first appears increases with increasing reduced frequency. Indeed for $k_r = 0.15$ the shock wave develops very late in the acceleration phase, see

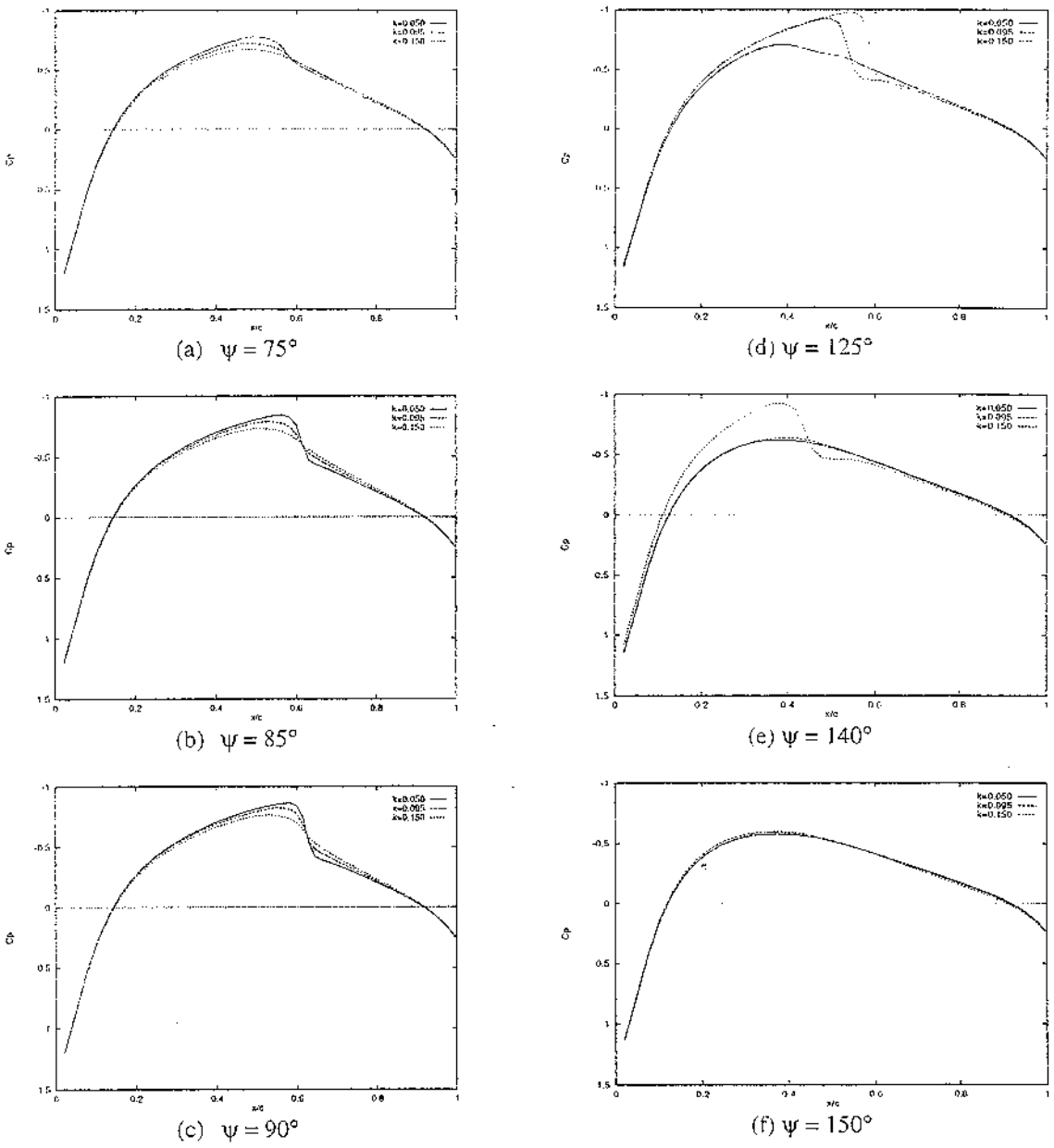

Figure (11) Influence of reduced frequency on the shock dynamics

Figure (11b) and at the azimuth angle for which the Mach number is a maximum, the shock is still very weak, see Figure (11c). Corresponding behaviour is observed at later azimuth angles. As reduced frequency is increased the shock wave persists until much later times in the flow development. At the lower reduced frequency ($k_r = 0.05$) the shock wave is no longer present for azimuth angles beyond $\psi = 125°$. In contrast for $k_r = 0.15$ the shock wave is still present for azimuth angle upto $\psi = 150°$, by which time the instantaneous Mach number has fallen to M = 0.646, well below the critical Mach number for this aerofoil section.

5.2 Indicial motion

The unsteady response of the flow around a NACA 0012 aerofoil set at 2° incidence to the freestream was calculated for step changes in Mach number of $\Delta M = \pm 0.01$ at several Mach numbers in the range $0.2 \leq M \leq 0.6$. The Reynolds number based upon chord was held constant at Re_c = 1 million. The calculated normal force response is shown in Figure (12). Here the forces are normalised by their final values and S is a non-dimensional measure of time (s = t U/c) which can be interpreted as the number of chord lengths travelled by the aerofoil.

For low Mach numbers a large initial pulse dominates the aerodynamic loading. This pulse is

associated with the system of disturbance waves generated by the instantaneous change in boundary condition at the aerofoil surface. The form of the calculated indicial response can be approximated using an exponential function of the general form,

$$C_N(t) = \frac{dC_N}{dM}\Delta M\left(1 - \sum_n A_n e^{-t/T_n}\right) \qquad (19)$$

where the constants A_n and T_n are to be determined.

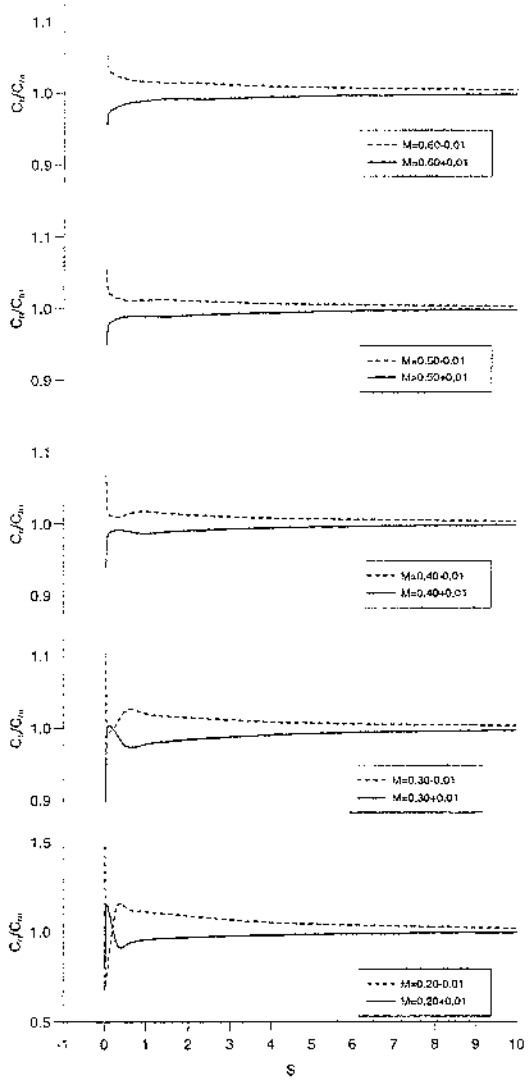

Figure (12) Computed flow response to a step change in Mach number (Indicial motion)

At the present time, there is no generalised model for these constants and they must be determined on a case by case basis. However, the assumed form is useful in determining the functional form of the response to harmonic forcing. As discussed by Beddoes[18] the response to arbitrary forcing can be determined using the step response and Duhamels integral. Using the assumed form of the response function, explicit solutions for the response to harmonic forcing can be obtained by transformation between the Laplace and time domains. This is done in Appendix A. The normal force response to harmonic forcing is found to be of the general form,

$$C_N(t) = M_o \frac{dC_N}{dM}\left(1 + \sum_n B_n \sin(\omega t + \phi_n)\right) \qquad (20)$$

in which the phase lag, ϕ, is determined from,

$$\tan(\phi_n) = \frac{1}{\omega T_n}$$

This expression is independent of the advance ratio, confirming the results obtained previously for harmonic oscillations.

6. Conclusions

The results of a numerical investigation of the unsteady aerodynamics associated with the blade sections of non-lifting helicopter rotors in forward flight was presented. The unsteady flow was studied through solutions of the two-dimensional Reynolds averaged Navier-Stokes equations together with a strongly coupled two-equation model of turbulence. The aerodynamic response to both harmonic and inidicial motion was studied.

For harmonic forcing, the influence of advance ratio and reduced frequency was investigated. The computed resulfs show that, in the absence of shock waves, the flow is periodic with a reduced frequency equal to that of the forcing motion. The computed response is harmonic in character, but lags behind the forcing motion. For constant reduced frequency, the results suggest that the phase lag between the forcing motion and the computed response is independent of advance ratio.

In addition to harmonic motion, the aerodynamic response to a step change in Mach number was investigated. The computed response functions to step forcing are similar in nature to those obtained for step changes in incidence. Using an assumed exponential form of the indicial response, a lift transfer operator for step changes in Mach number was obtained in the Laplace domain. An analytical expression for the response to harmonic Mach number oscillations was then obtained from the transfer operator. The resulting formulation for the aerodynamic response is independent of the advance ratio, confirming the previous findings for the harmonic motion.

Acknowledgements

The work described in this paper was funded by the Engineering and Physical Science Research Council (EPSRC) Managed Programme in Aerodynamics. The authors are grateful to Mr J. Perry (Chief Aerodynamicist) and Dr. A. Kokkalis (CFD

Specialist) of GKN Westland Helicopters Ltd for their support.

References

1. Buchtala, B, Wehr, D. and Wagner, S. 'Coupling of aerodynamic and dynamic methods for the calculation of helicopter rotors in forward flight', Proceedings of the 23rd European Rotorcraft Forum, September 1997.
2. Maresca, C., Favier, D. and Rebont, J., 'Experiments on an aerofoil at high angle of incidence in longitudinal oscillations', J. Fluid Mechanics, Vol. 92 (4), 1979.
3. Krause, E. and Schweitzer, W.B., 'The effect of an oscillatory free-stream-flow on a NACA-4412 profile at large relative amplitudes and low Reynolds numbers', Experiments in Fluids Vol. 9 (1190), pp. 159-166.
4. Gursul, I. And Ho, C-M., 'High aerodynamic loads on an airfoil submerged in an unsteady stream', AIAA J., Vol. 30(4), 1992, pp. 1117-1119.
5. Shi, C. and Ho, C-M., 'Vorticity balance and time scales of a two-dimensional airfoil in an unsteady freestream', Phys. Fluids, Vol. 6(2), 1994, pp. 710-23.
6. Gursul, I., Lin, H. and Ho, C-M., 'Effects of time scales on lift of airfoils in an unsteady stream', AIAA J., Vol. 32(4), 1994, p.797-801.
7. Morinishi, K. and Muratu, S., 'Numerical solutions of unsteady oscillating flows past an airfoil', AIAA Paper 92-3212, 1992.
8. Szumowski, A.P., and Meier, G.E.A., 'Forced oscillations of airfoil flows', Experiments in Fluids, Vol. 21, 1996, pp.457-64.
9. Tidjeman, H. 'Investigation of the transonic flow around oscillating aerofoils', NLR Report TR 77090U, 1977.
10. Lerat, A. and Sides, J., 'Numerical simulation of unsteady transonic flows using the Euler equations in integral form', ONERA, TP 1979-10, 1979.
11. Habibie, I.A., Laschka, B. and Weishaupl, C., 'Analysis of unsteady flows around wing profiles at longitudinal accelerations', Proceedings of the 19th International Congress of the Aeronautical Sciences, pp. 2692-2704, 1994.
12. Lin, C.Q. and Pahlke, K., 'Numerical solution of the Euler equations for aerofoils in arbitrary unsteady motion', Aeronautical Journal, June/July 1994.
13. Pahlke, K., Blazek, J. and Kirchner, A., 'Time accurate Euler computations for rotor flows', RaeS Conference on CFD, Paper 15, 1994.
14. Shaw, S.T. and Qin, N., 'Solution of the Navier-Stokes equations for the flow around an aerofoil in an oscillating freestream', Proceedings of the 20th congress of ICAS, Sorrento, 1996.
15. Shaw, S.T. and Qin, N., 'Solution of the Navier-Stokes equations for aerofoils undergoing combined translation pitch oscillations', 22nd European Rotorcraft Forum, Brighton, September 1996.
16. Shaw, S.T. and Qin, N., 'Unsteady flow around helicopter rotor blade sections in forward flight', Aeronautical Journal, Vol. 103(1019), January 1999.
17. Shaw, S.T., 'Numerical study of the unsteady aerodynamics of helicopter rotor aerofoils' PhD Thesis, Cranfield University, 1999.
18. Beddoes, T.S., 'Practical computation of unsteady lift', Vertica, Vol. 8(1), 1984.
19. Shaw, S.T. and Qin, N. 'Numerical prediction of the aerodynamic response of aerofoils subjected to step increases in Mach number', 23rd European Rotorcraft Forum, Dresden, September 1997.
20. Wilcox, D.C., 'Turbulence modelling for CFD', DCW Industries Inc., 1993.
21. Qin, N., Ludlow, D.K., Shaw, S.T. and Richardson, G., 'A unified high resolution approach for two equation turbulence modelling', Proceedings of the 3rd Pacific International Conference on Aerospace Science and Technology, p.219, 1997
22. Osher, S. and Solomon, F., "Upwind difference schemes for hyperbolic systems of conservation laws", Mathematics of Computation, Volume (38), Number 158, April 1982, pp. 339-374.
23. Van Leer, B., Van Leer, B., 'Towards the ultimate conservative difference scheme V: A second order sequel to Godunov's method', J. Comp. Physics, Vol. 32, pp. 101-136, 1979.
24. Saad, Y. and Schultz, M.H., 'GMRES: A generalised minimal residual algorithm for solving non-symmetric linear systems', SIAM J. Sci. Stat. Comp., Vol. 7(3), pp. 856-869, 1986.
25. Badcock, K.J., Xu, X., Dubuc, L. and Richards, B.E., 'Preconditioners for high speed flows in aerospace engineering', Numerical Methods for Fluid Dynamics V., Oxford University Press, 1996, pp. 287-94.
26. Landon, R.H., 'NACA 0012 oscillatory and transient pitching', Paper 3, AGARD R-702, 1982.
27. Gaitonde, A.L., Jones, D.P. and Fiddes, S.P., 'A 2D Navier-Stokes method for unsteady compressible flow calculations on moving meshes', Aeronautical Journal, Vol. 102(1012), 1998.
28. Badcock, K.J., and Gaitonde, A.L., 'An unfactored implicit moving mesh method for the two-dimensional unsteady N-S equations', Int. J. For numerical methods in fluids, Vol. 23, 1996, pp. 607

29. Singh, R. and Baeder, J.D., 'Direct Calculation of Three-dimensional Indicial Lift Response Using Computational Fluid Dynamics', J. Aircraft, Vol. 34(4), 1997.
30. Mazelsky, B. and Drischler, J.A., 'Numerical determination of indicial lift and moment functions for a two-dimensional sinking and pitching airfoil at Mach numbers 0.5 and 0.6', NACA TN 2739, 1952.

Appendix A

The character of the indicial response functions calculated for a step increase in Mach number is similar to that obtained for a step increase in incidence[18]. It should therefore be possible to represent the response in the approximate form,

$$C_N = \frac{dC_N}{dM}\overline{M}\left(1-\sum_n A_n e^{-t/T_n}\right) \qquad (A1)$$

where $\overline{M}$ is the step change in Mach number and A_n and T_n are constants which must be determined. The constants A_n are subject to the constraint $\sum_n A_n = 1$.

Using this assumed form the transfer function can be obtained by transformation to the Laplace domain thus,

$$\frac{C_N(s)}{M(s)} = \frac{dC_N}{dM}\left(1-\sum_n A_n + \sum_n \frac{A_n}{(1+sT_n)}\right) \qquad (A2)$$

and the normal force for an arbitrary variation of Mach number can be found from,

$$C_N(s) = \frac{dC_N}{dM}\left(\sum_n \frac{A_n}{(1+sT_n)}\right)M(s) \qquad (A3)$$

For a sinusoidal variation of Mach number about a mean value M_o the forcing function in the Laplace domain is,

$$M(s) = M_o\left(\frac{1}{s}+\frac{\mu\omega}{s^2+\omega^2}\right) \qquad (A4)$$

and the normal force is given by,

$$C_N(s) = M_o\frac{dC_N}{dM}\left(\sum_n \frac{A_n}{(1+sT_n)}\right)\left\{\frac{s^2+\omega^2+\mu\omega s}{s(s^2+\omega^2)}\right\} \qquad (A5)$$

which can be written in terms of partial fractions as,

$$C_N = M_o\frac{dC_N}{dM}\left\{\sum_n \frac{A_n}{s}+\frac{\pi_{1,n}+\pi_{2,n}s}{s^2+\omega^2}+\frac{\pi_{3,n}}{1+sT_n}\right\} \qquad (A6)$$

Taking the inverse transform and $t \to \infty$ we obtain the following form for the unsteady normal force due to the prescribed motion,

$$C_N(t) = M_o\frac{dC_N}{dM}\left(1+\sum_n \frac{\pi_{1,n}}{\omega}\sin(\omega t)+\pi_{2,n}\cos(\omega t)\right)$$

with,

$$\pi_{1,n} = \frac{1}{T_n}\frac{\mu\omega A_n}{(T_n^2+\omega^2)} \quad \text{and} \quad \pi_{2,n} = -\frac{\mu\omega A_n}{(T_n^2+\omega^2)}$$

This expression can be simplified to obtain the following expression for the unsteady normal force coefficient,

$$C_N(t) = M_o\frac{dC_N}{dM}\left(1+\sum_n B_n\sin(\omega t+\phi_n)\right) \qquad (A7)$$

where the phase angle ϕ_n is obtained from the ratio of the constants $\pi_{1,n}$ $\pi_{2,n}$ using,

$$\tan(\phi_n) = \frac{\pi_{1,n}}{\omega\pi_{2,n}} = -\frac{1}{\omega T_n} \qquad (A8)$$